ISSN 2029-6991 / eISSN 2029-7009

GEODESY and CARTOGRAPHY

2025
Volume 51
Issue 2
Pages 67–80
https://doi.org/10.3846/gac.2025.23771

UDC 528.931.2

DROUGHT SAFETY LEVELS ASSESSMENT IN UZBEKISTAN PART OF THE KHOREZM OASIS BY GEOSPATIAL METHODS

Muzaffar MATCHANOV[1✉], Matías MUDARRA[2], Askar NIGMATOV[3], Rifat BOYMURODOV[4], Ruslan JUMABAYEV[1], Ali HAKIMI[5], Otabek MATCHANOV[1]

[1]Geodesy, Cartography and Cadastre Department, Faculty of Technics, Urgench State University named after Abu Rayhan Biruni, Urgench, Uzbekistan
[2]Centre of Hydrogeology of the University of Malaga (CEHIUMA), Malaga, Spain
[3]General Professional Sciences Department, Academy of Labour and Social Relations, Tashkent, Uzbekistan
[4]Geography Department, Faculty of Natural and Agricultural Science, Urgench State University named after Abu Rayhan Biruni, Urgench, Uzbekistan
[5]Department of Physical Geography and Ecosystem Sciences, Lund University, Lund, Sweden

Article History:
- received 23 April 2024
- accepted 28 May 2025

Abstract. The issue of drought has emerged as a significant challenge in the Khorezm oasis over recent decades. Furthermore, the construction of the Kushtepa canal in Afghanistan is expected to exacerbate the impact of drought in the region. It is of the utmost importance to evaluate the resilience of the oasis to drought in order to ensure effective planning and mitigation strategies. This study employed geospatial data, including the normalized difference of vegetation index (NDVI), land surface temperature (LST), normalized difference of moisture index (NDMI), soil brightness, groundwater table, digital elevation model (DEM), and distance to Amudarya river, derived from Landsat 5 TM, and Landsat 8 OLI/TIRS data (2000–2023). A weighted overlay analysis was employed to identify the most influential factors, which were found to be distance from the river, canal density, soil brightness, LST, and groundwater table. The findings indicate that 3746 km^2 of the oasis is safe, while 4644.32 km^2, 5563.77 km^2, 5486.17 km^2, 7832.64 km^2 are classified as dangerous, mid dangerous, high dangerous, and extreme dangerous, respectively. It is recommended that agricultural use be prioritised in areas deemed safe, that construction be restricted, and that population migration from high-risk regions to safer areas be facilitated.

Keywords: drought, LST, the main canals' density, groundwater table, distance from Amudarya, drought safety levels assessment map.

✉Corresponding author. E-mail: *mmuzaffar@yandex.ru*

1. Introduction

The term "drought" is defined as a period of deficient moisture conditions that disrupts normal climatological and hydrological conditions. These conditions are influenced by a combination of natural and anthropogenic activities. Droughts are classified by researchers into three main categories: meteorological, agricultural, and hydrological (Hosseinzadehtalaei et al., 2023; Chen et al., 2022). Other forms of drought, including those of an anthropogenic and ecological nature, have also been the subject of research (Wilhite & Glantz, 1985). Drought is a distinctive type of disaster with multifaceted impacts on human life and the natural environment. The impacts of drought can be wide-ranging and include water shortage, hunger, the spread of various diseases, an increased risk of insect infestations, desertification, reduced soil fertility and lower crop yields (Lloyd-Hughes, 2014; Shah & Mishra, 2020). Moreover, the periodic and spatial characteristics of droughts, in conjunction with their continuous nature, contribute to the complexity of studying, preparing for and mitigating the negative effects of droughts (Wu et al., 2013).

A number of geospatial technologies have been successfully employed in the assessment of droughts, with several methods proving particularly effective (Dubey et al., 2023; Das et al., 2023; Van Loon et al., 2022; Raczynski & Dyer, 2022). McKee et al. (1993) introduced the Standardized Precipitation Index (SPI), which identifies precipitation levels below the normal range as key indicators of drought. However, in the Khorezm region, where the mean annual rainfall is only 160 mm, the SPI method may not be the most effective approach for assessment. In their respective studies, Jang (2018) and Zarei (2018) employed the reconnaissance drought index (RDI), incorporating potential evapotranspiration (PET) as an indicator. However, in the context of the 2000-year drought in the oasis, no significant correlation was observed between PET and soil moisture. In a recent study, Gonçalves et al. (2023) employed a range of drought assessment methods, including SPI, SWSI, EDDI, SDI, and RDI, in semi-arid regions of Brazil, thereby demonstrating the utility of diverse approaches in this context. Baniya et al. (2019) proposed the use of the Vegetation Condition Index (VCI) as a means of evaluating drought, with particular emphasis on vegetation cover as a key indicator. However, in the Khorezm oasis, vegetation cover is a consequence rather than a factor influencing the situation. As observed by Hao et al. (2017), the occurrence, impacts and preparedness strategies for drought vary across regions, emphasising the necessity for a bespoke drought assessment methodology that is specific to the geographic characteristics of the oasis. This work aims to develop a drought assessment methodology for the Khorezm oasis and understand its territorial features. Additionally, the distribution of safety levels in relation to drought conditions and formulation recommendations to mitigate its deleterious impacts were also planned.

2. Materials and methods

2.1. Study area

The Khorezm oasis is a 31 885.41 km^2 geographic region situated between the Qyzylkum and Qaraqum deserts in Central Asia (Matchanov et al., 2016; Boymurodov et al., 2024). The size of the oasis is susceptible to fluctuations due to an inherently unstable irrigation water regime. It is recommended that drought assessments be conducted during June and July, when irrigation water demand for agriculture and vegetation is at its highest, and the impact of drought also is most severe. The climate of the oasis is arid (the highest annual mean temperature +28 °C), characterised by low precipitation levels (92 mm) and high rates of evapotranspiration. The region's economy is significantly reliant on the Amudarya river's water flow. Therefore, factors such as LST, NDMI, NDVI, and groundwater table becomes consequence factors that in the assessment of drought conditions. The proximity of the river and the density of the main irrigation canals exert a main influence on the vegetation cover of the oasis. The region of Khorezm has a long history of irrigational agriculture, with over three millennia of experience and a landscape that has been shaped by intensive land use. As a result, droughts have a deleterious effect on the population's income and quality of life, as evidenced by the 2000, 2001, 2008, and 2012 severe droughts. Furthermore, contradictory events, such as floods in small canals (Mansourian et al., 2023) also impact the region.

2.2. Data

A variety of techniques were used employed in the collection and preparation of geospatial data. The principal canals were digitized from highly accurate analog topographic maps. The line densities were subsequently calculated then and a raster with a density of km. kv/m was created.

The annual mean LST data, covering the years 2000–2023, were downloaded from the Climate Engine platform and mosaiced into a new raster (Climate Engine, 2023). The Landsat 4-5 TM (band 6), Landsat 8 OLI/TIRS (bands 10, 11) data were used to calculate LST, using the following formula:

$$LST = Tb/[1 + (\alpha \times Tb / C2) \times \ln(\varepsilon)]$$ (Tajudin et al., 2021).

The NDVI has been a popular index in research projects assessing droughts (Brown et al., 2008; Crippen, 1990; Gorelick et al., 2017). Defining an appropriate time for NDVI-drought analysis is typically dependent on a few factors, including geographical region, specific characteristics, and the type of the drought. In the Khorezm oasis, drought reached a dangerous level in July, a period when plants and agricultural fields require substantial irrigation. The annual mean NDVI data covering 2000 to 2023 were downloaded from the same platform which cited above and mosaiced into a new raster (Climate Engine, 2023). Landsat 4-5 TM (bands 3, 4), Landsat 8 OLI/TIRS (bands 4, 5) data were used to calculate the NDVI values, using the established formula (Crippen, 1990):

$$NDVI = (B04 - B03) / (B04 + B03), \text{ Landsat 4-5 TM;}$$

$$NDVI = (B05 - B04) / (B05 + B04), \text{ Landsat 8 OLI/TIRS.}$$

Landsat 4-5 TM, Landsat 8 OLI/TIRS data from 2000 to 2023 were downloaded from Google Earth Engine platform (Gorelick et al., 2017) and used to calculate NDMI using the following formulas (Gao, 1996):

$$NDMI = (B04 - B05) / (B04 + B05), \text{ Landsat 4-5 TM;}$$

$$NDMI = (B05 - B06) / (B05 + B06), \text{ Landsat 8 OLI/TIRS.}$$

Soil brightness, which is influenced by a range of earth features (Salleh et al., 2014), has also been employed by some researchers as a means of detecting drought (Wang et al., 2004; Yao et al., 2008). Consequently, soil brightness was calculated from thermal bands of Landsat 4-5 TM and Landsat 8 OLI/TIRS from 2000 to 2023, downloaded from Earth Explorer database, using the following formulas (Li et al., 2004; Schneider & Mauser, 1996):

$$TB = (k^2 / \ln[k^1 / I\lambda(0) + 1]).$$

Landsat 4-5 TM: $k^1 = 607.76$ Wm^{-2} sr^{-1} μm^{-1}, and $k^2 = 1260.56$ K.
Landsat 8 OLI/TIRS: $k^1 = 480.89$ Wm^{-2} sr^{-1} μm^{-1}, and $k^2 = 1201.14$ K.
k^1 and k^2 are correction coefficients.

The annual mean groundwater table (AMGWT), typically obtained through field observations, was identified as a crucial element in the assessment of drought conditions in the case of the oasis. However, it is also a result factor formed by Amudarya river flow, with a decrease to between 5 and 10 meters observed during the drought years of 2000 and 2001. The data were gathered from by ZEF/UNESCO project (1990–2004) and from hydrogeological stations in Khorezm and Karakalpakstan (2018–2021). The point data were averaged and converted into raster data by IDW interpolation methods.

The researchers also employed DEM data to examine drought (Dubey et al., 2023; Mirmohammad Hosseini et al., 2020). This data originated from the SRTM database (NASA JPL, 2020) and, when compared to other open-source DEM data, demonstrated greater accuracy even in small agricultural regions (Matchanov, 2020).

The impact of rivers on drought was demonstrated by researchers (Van Loon et al., 2022; Raczynski & Dyer, 2022). This factor was of great consequence for the study area, as the existence of the oasis was contingent upon the flow of the Amudarya river. The Takhiatash hydro post was selected as the river's terminus, beyond which the river's water was fully distributed to canals. Buffer zones were established to quantify distances from the Amudarya river. Each buffer distance was calculated based on the field observations during the 2000 drought and under normal conditions in 2022, utilizing LST, NDVI, and NDMI values. The following Landsat 5 TM and Landsat 8 OLI/TIRS data were employed to make comparisons and to analyse correlations (Table 1). The negative effects of drought are most evident and reach their maximum in July. Therefore, it is possible to determine the weight of the influencing indicators in July.

Table 1. Landsat images used

Name	Data features
Landsat 5 TM	LT05_L1TP_159031_20000723_20161214_01_T1
	LT05_L1TP_160030_20000730_20180922_01_T1
	LT05_L1TP_160031_20000730_20180922_01_T1
	LT05_L1TP_161030_20000721_20180913_01_T1
Landsat 8 OLI/TIRS	LC08_L1TP_159031_20220720_20220726_02_T1
	LC09_L1TP_160030_20220719_20230406_02_T1
	LC08_L1TP_160031_20220711_20220722_02_T1
	LC08_L1TP_161030_20220718_20220726_02_T1

2.3. Methodology

The methodology employed in this study is illustrated in Figure 1. The influence of the indicators on the drought was assessed in comparison between the drought in year of 2000 and normal year of 2022. This comparison facilitated the identification of the primary, secondary, and other indicators that exerted a significant influence on the situation.

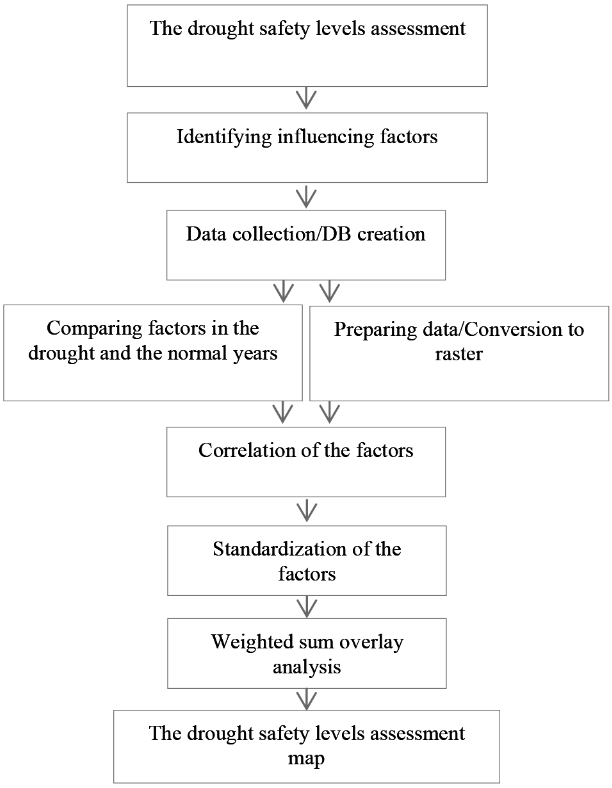

Figure 1. General workflow methodology for the drought safety levels assessment

3. Results and discussion

3.1. Correlations

The correlations between the influencing and consequence indicators were subjected to analysis in the following manner. The density of canals was a pivotal factor in the provision of irrigation water to agricultural fields, exerting a considerable influence on soil moisture and temperature, the water balance of wetlands, vegetation cover, and the needs of the local population. There was a relationship between the density and LST for the months of July in both 2000 and 2022 (Figure 2a, 2b). A negative correlation was identified between those two factors, with correlation coefficients of –0.49 and –0.57 for the two years 2000 and 2022. This indicated that as the density of canals increased, the LST values decreased. In both years, high-temperature points of 50 °C were observed in areas where the density of the main canals was higher (when 1 km sq. has 200–300 meters canals). The aforementioned points indicated that no agricultural activities were conducted in the selected fields during the specified years.

In the 2000 drought, areas with low soil temperatures were primarily observed in regions with very low canal density. As a result of more consuming groundwater by more utilized farmers (Figure 3a, 3b). To further investigate this, we tested the correlation between the AMGWT and land surface temperature (LST) (Figure 2c, 2d). The results in Figure 2c showed no significant correlation during the 2000 drought. To determine where these correlations were absent, HotSpot method was applied (Getis & Ord, 1992) (Figure 3c, 3d). The non-significant points identified in the HotSpot maps were compared with aerial photos, NDVI values, and experimental field data. The analysis confirmed that groundwater was used for agriculture in these areas, explaining the lower LST values in regions where the groundwater level was also low. However, due to high costs, not all farmers could access this water. As shown in Figure 3, groundwater was consistently used across all tested years in the Khorezm region of the oasis.

It can be theorized that as the AMGWT rises closer to the surface, increased evapotranspiration leads to a decrease in surface temperature. This hypothesis was supported by observations from the oasis in both 2000 and 2022. The correlation between AMGWT and LST was 0.29 in 2000 and 0.45 in 2022, indicating a weaker relationship during the 2000 drought. During the drought, farmers relied on groundwater for irrigation, leading to surface temperatures reaching 35–45 °C in areas where the AMGWT was recorded at 3.5–4.5 meters (Figure 2c, 2d). The HotSpot analysis identified cold spots in non-agricultural areas in the southern part of the oasis (Figure 3c, 3d). In these regions, the AMGWT was closer to the surface due to the natural decrease in elevation towards the south and southwest, which directed both ground and surface water flow in that direction. Additionally, the correlation between canal density and AMGWT was weaker due to these hydrological conditions (Figure 2e). The Khorezm region, in particular, exhibited a higher groundwater table compared to the Karakalpakstan region (Figure 3e, 3f). However, during the 2000 and 2001 droughts, groundwater levels declined significantly to 5–10 meters, highlighting the impact of prolonged drought conditions and other environmental factors. Additionally, canal density showed a correlation with NDMI in both years, emphasizing its role in water distribution and drought mitigation.

There were no correlation between NDVI and the main canals' density (0.01), AMGWT (0.01), or LST (–0.01) during the drought of 2000. These values were slightly higher in 2022, with correlations of 0.44, –0.29, and –0.78 respectively. The correlation values for all other indicators were similar in 2022 (Table 2).

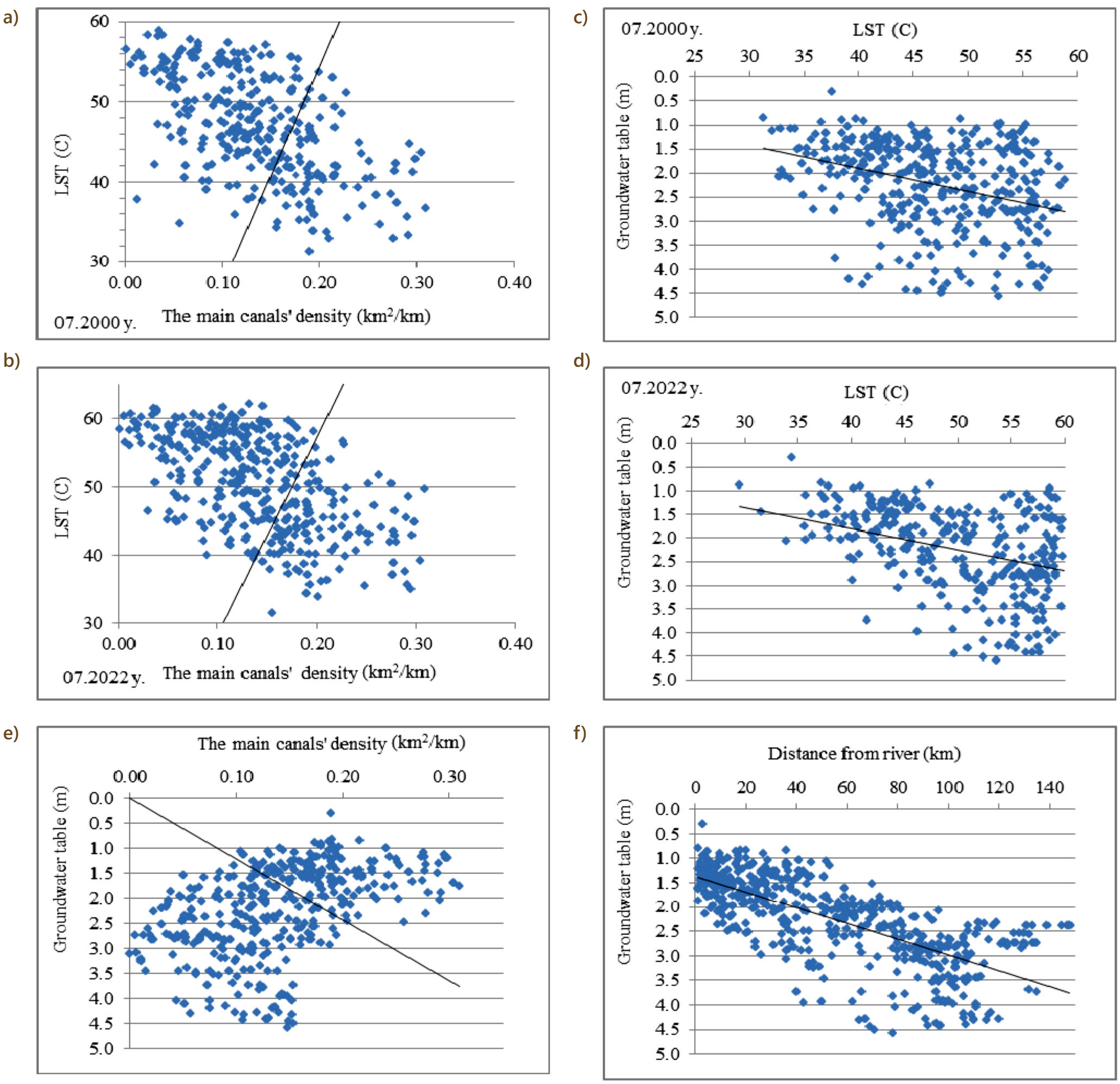

Figure 2. Correlations of factors that were used for drought assessment

The findings indicate that the density of the main canals and the Amudarya River play a pivotal role in influencing drought conditions in the oasis. Furthermore, the river exerts a substantial impact on the AMGWT within the region (Figure 2f).

The correlation between soil brightness and LST was stronger in both years. This is likely due to the fact that both indicators were calculated from the same Landsat 5 TM and 8 OLI/TIRS bands. Furthermore, regions exhibiting adequate moisture levels demonstrated lower soil brightness values. Once more, the density of canal was found to exert a considerable influence on these factors too. NDMI which indicates the moisture content of vegetation (Gu et al., 2008; Assal et al., 2016), demonstrated

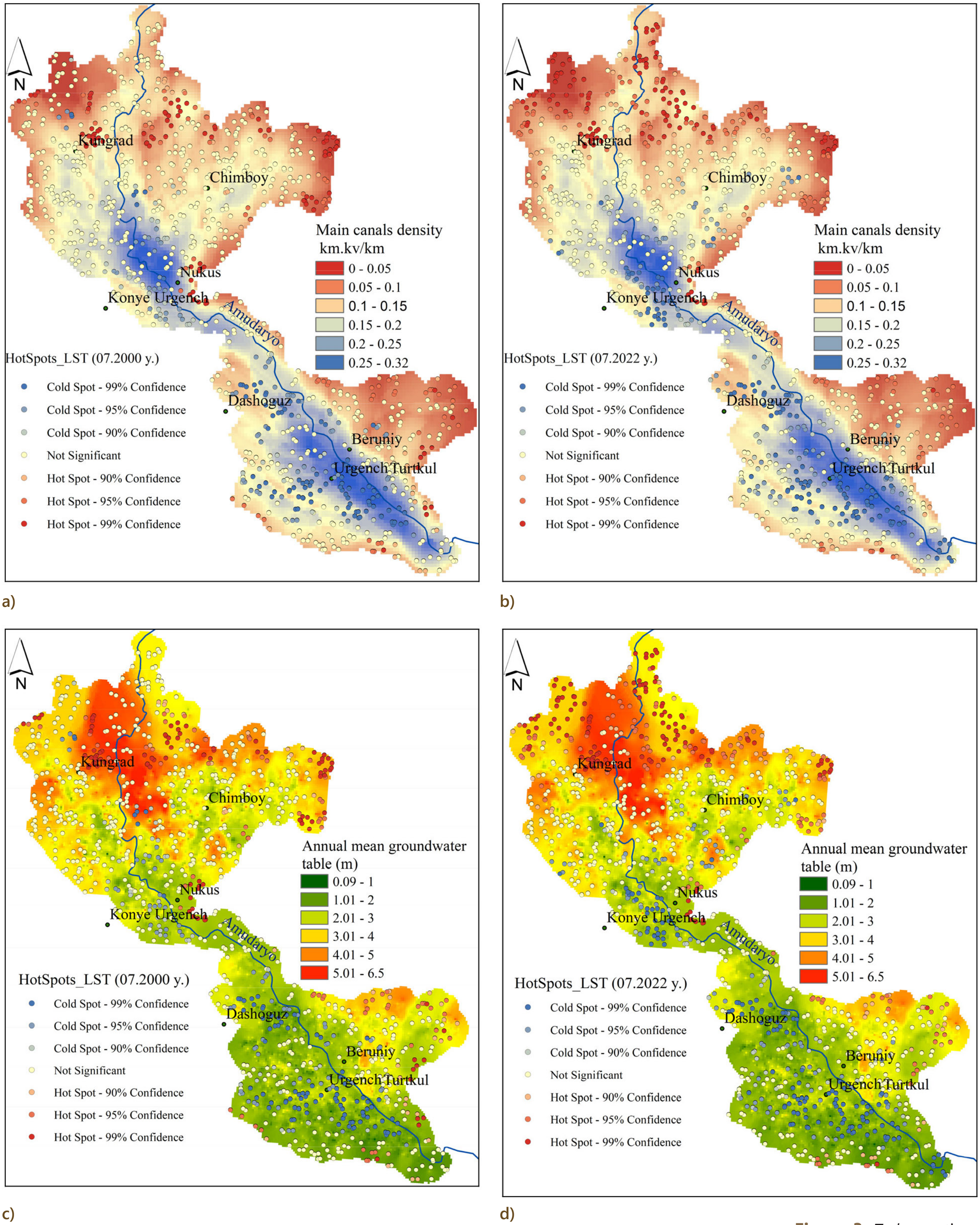

Figure 3. *To be continued*

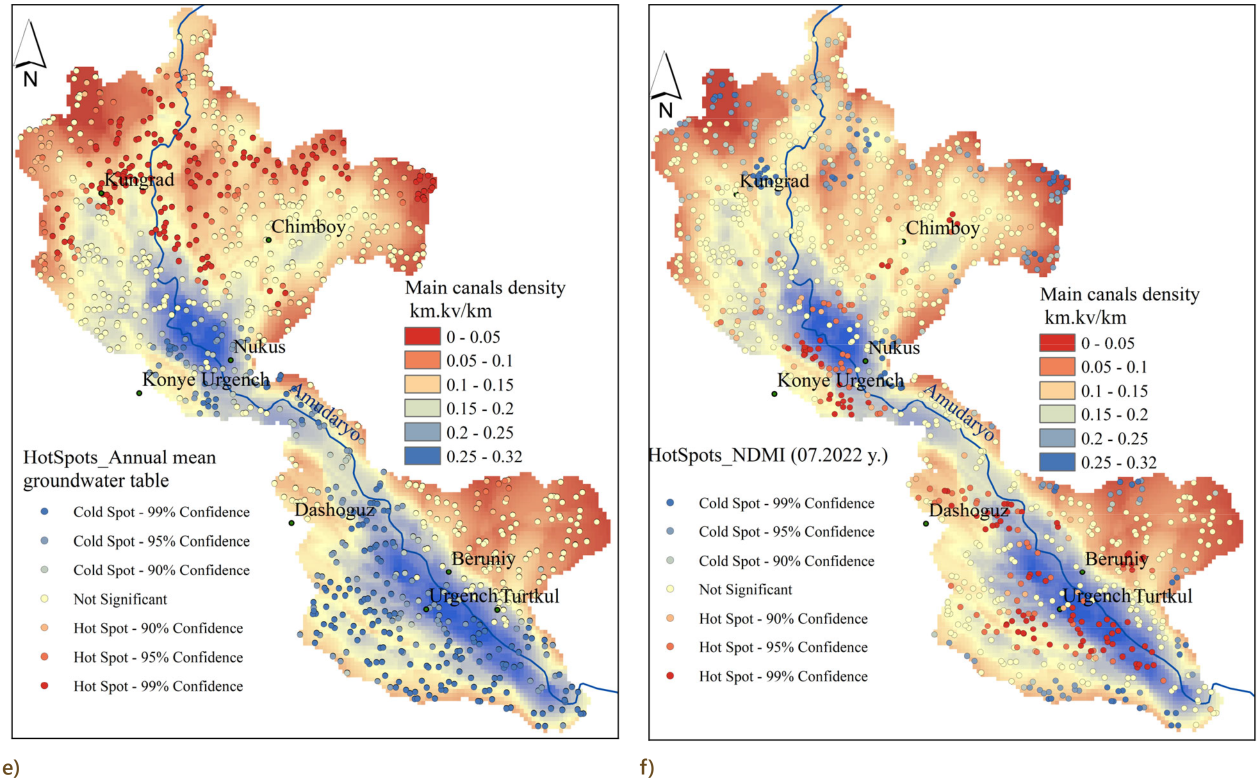

Figure 3. Hot Spot analysis of LST, the main canals' density, NDMI, and the AMGWT

Table 2. Correlation table of indicators influencing the drought in 2000 and 2022 years

2022 year

	LST 22.07	NDVI 22.07	CANALS DENS	AMGWT	DEM SRTM	Soil brightness	Distance river	NDMI
LST_22.07	1							
NDVI 22.07	–0.78	1						
CANALS_DENS	–0.57	0.44	1					
AMGWT	0.45	–0.29	–0.46	1				
DEMSRTM	–0.18	0.02	0.19	–0.55	1			
SoilBrightness	0.95	–0.78	–0.52	0.45	–0.16	1		
Distance_River	0.52	–0.34	–0.58	0.72	–0.68	0.48	1	
NDMI	–0.81	0.91	0.45	–0.27	0.00	–0.79	–0.31	1

2000 year

	LST 20.07	NDVI 20.07	CANALS DENS	AMGWT	DEM SRTM	Soil brightness	Distance river	NDMI
LST20.07	1							
NDVI 20.07	–0.01	1						
CANALS_DENS	–0.49	0.01	1					
AMGWT	0.29	0.01	–0.47	1				
DEMSRTM	–0.08	0.00	0.20	–0.55	1			
SoilBrightness	0.84	–0.03	–0.43	0.1	0.07	1		
Distance_River	0.36	–0.02	–0.59	0.72	–0.69	0.10	1	
NDMI	–0.87	0.01	0.41	–0.17	–0.04	–0.77	–0.24	1

a stronger correlation with NDVI in 2022 year and no correlation during the 2000 drought. Additionally, NDMI exhibited a weak positive correlation with canal density in both drought and normal years (Table 2; Figure 3f).

As demonstrated in Table 2, all factors exerted a degree of influence on the drought. The weakest factor was SRTM DEM, which demonstrated only a significant correlation with the AMGWT. However, the DEM played a significant role in the Khorezm region part of the study area, where a reduction in elevation groundwater becoming more accessible. This resulted in the formation of numerous lakes and wetlands, which in turn led to an increase in vegetation cover in the southern regions. Based on the aforementioned observations, the following sequence of influences can be proposed for assessment: distance from the river, main canal density, soil brightness, LST, AMGWT, NDVI, NDMI, and DEM.

3.2. Assessment

In order to evaluate the impact of drought conditions on the oasis, a weighted overlay technique were employed. Initially, all factors were converted to raster with an identical pixel size. Subsequently, each factor was assigned a grade on a scale of 1–5, based on field observations, conditional spatial autocorrelations, and comparisons between the years 2000 and 2022 (Table 3). The safety levels were chosen conditionally. The presence of any amount of threats indicates that the situation on the ground is unsafe. Therefore, even a good NDVI value of 0.5–0.7 corresponds to a dangerous situation in the oasis.

The grades and levels for each factor were assigned specific, conditional, and equal values in accordance with the prevailing circumstances. The safe level for the 10 km distance from the river was indicated by the presence of stable and dense vegetation cover (NDVI 0.6), continuous LST below 35 °C (from 2000–2022), a main canal density of 250–320 meter/km^2, and uninterrupted distribution of annual mean groundwater table up to 2 meters (Figure 4a).

However, the right bank of the river, the higher elevation resulted in slightly lower values for these factors, with NDVI ranging from 0.3 to 0.6 and a more variable LST. This geographic variation affected the grades of all factors across different parts of the oasis, necessitating a multi-criteria analysis. Field observations from the 2000 drought indicated that AMGWT decreased by an average of 0.5–1 m for every 20 km. At a distance of 10 km, AMGWT was recorded at 3.5–4 m, at 30 km it was 4–4.5 m, and at 50 km it was over 5 m.

Anthropogenic factors, including political influence, traditional agricultural practices, and local needs exerted a significant influence on the oasis. The aforementioned factors precluded the possibility of discerning clear distinctions in main canal densities. In practice, the oasis was entirely covered by a multitude of canal levels. The results of the field observations indicated that the main canals only had water available during drought years. Following a series of evaluations and comparisons, it was determined that equal intervals should be established for main canal density. Areas with densities of 250–320 meters/km^2 were found to correspond to locations within 10 km distance from of the river (Figure 4b). However, in the Chimbay region, the AMGWT was observed to be up to 2 meters AMGWT with a main canal density of 100–150 meters, which was similar to other 10 km distance area from the river. Therefore, subsequent levels of the main canal density were assigned conditional grades.

The grades for soil brightness were tested a variety of reclassification methods, including Natural Breaks, Equal Interval, Defined Interval, Quantile, Geometric Interval, and Standard Deviation. The Natural Breaks method provided the most logical, practical representation for physical geography, and land use justifications in the oasis (Figure 4c). The safe areas based on the soil brightness factor aligned with the safe areas identified for LST, NDVI, and NDWI. The buffer zones within 5 km around the oasis were classified as extreme-dangerous areas. The intermediate safety grades for other factors showed mixed and irregular patterns across the region.

In previous research, LST values were also employed for the assessment of drought conditions, with the selected values being informed by regional geography and the specific research objectives (Das et al., 2023; Patil et al.,

Table 3. The factors influencing to the drought: safety levels, weights, values and grades

	Weights								
	0.2	0.18	0.15	0.13	0.11	0.09	0.08	0.06	
Safety levels	Distance from the river (km)	The main canals density (km^2/km)	Soil brightness (%)	LST (°C)	AMGWT (m)	NDVI	NDMI	DEM	Grades
Safe	10	0.25–0.32	19.0–32.8	26.03–35	0.87–1.5	0.7–1	0.13–0.27	95–320	5
Dangerous	30	0.20–0.25	32.8–36.1	35–40	1.5–2	0.5–0.7	0.09–0.13	85–95	4
Mid-dangerous	50	0.15–0.20	36.1–39.4	40–45	2–2.5	0.3–0.5	0.05–0.09	75–85	3
High-dangerous	70	0.1–0.15	39.4–42.8	45–50	2.5–3.5	0.1–0.3	0.007–0.05	65–75	2
Extreme-dangerous	154	0–0.1	42.8–48	50–60.75	3.5–5	–0.06–0.1	–0.2–0.007	35–65	1

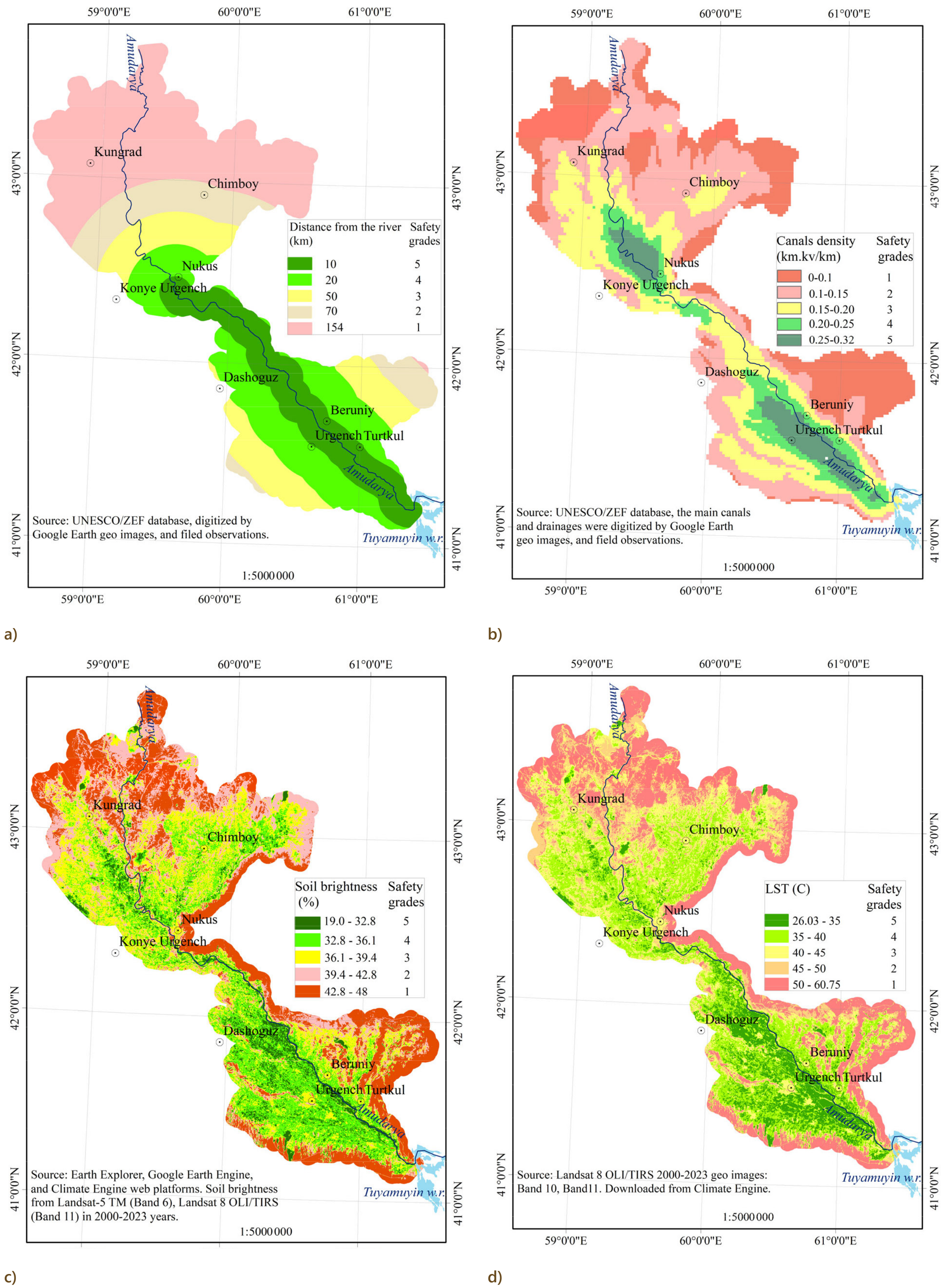

Figure 4. *To be continued*

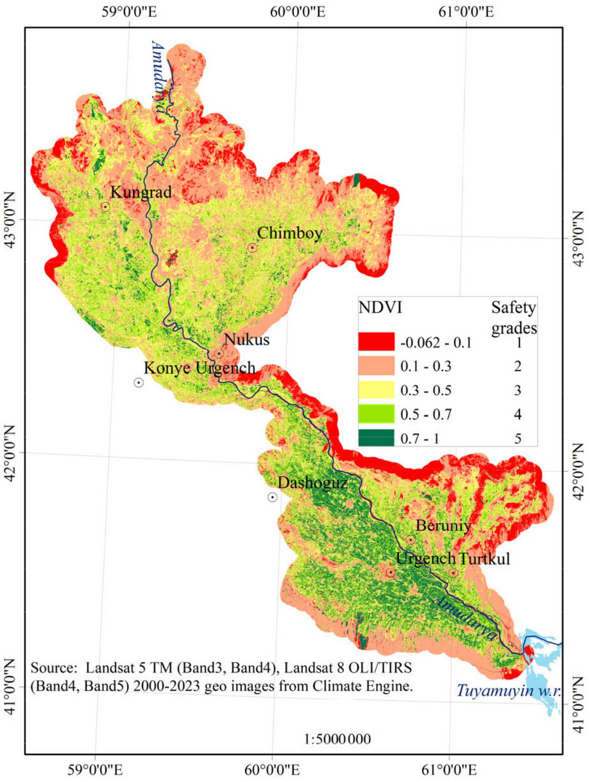

e)

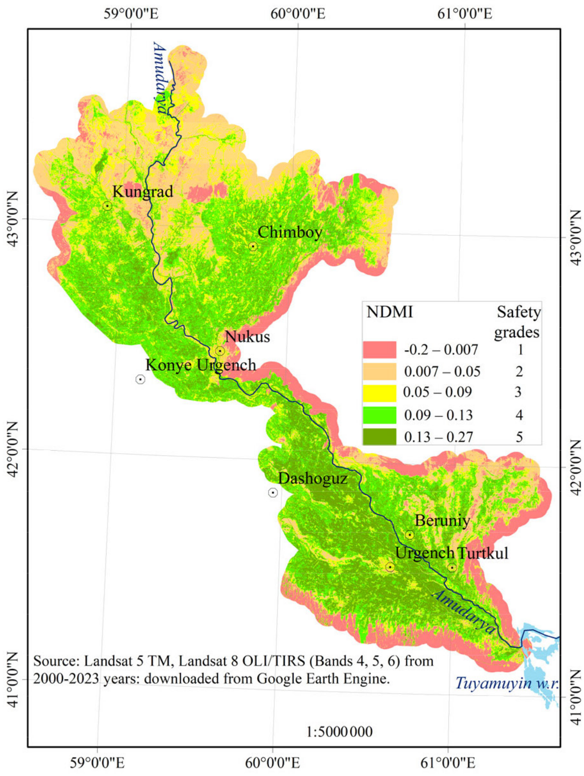

f)

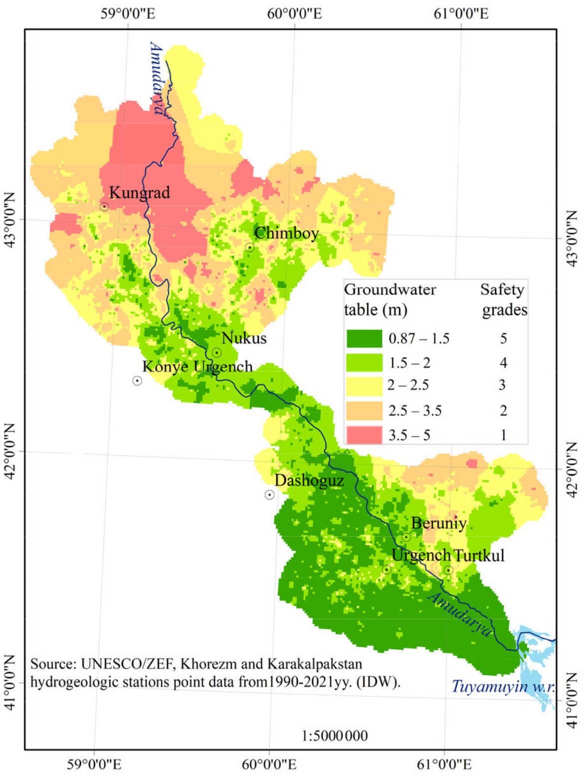

g)

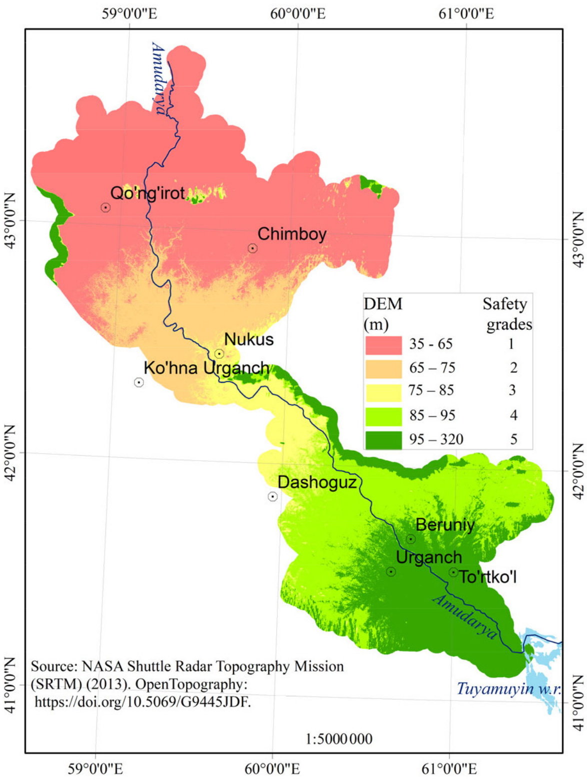

h)

Figure 4. Safety grades for distance from: a – the river; b – the main canals density; c – the soil brightness; d – LST; e – NDVI; f – NDMI; g – AMGWT; h – DEM

2021). In consideration of the oasis's location within an arid region, the safety levels higher threshold than in previous studies. A land surface temperature of up to 35 °C was deemed safe in this study (Figure 4d) due to the alignment of NDVI and NDMI safe areas within this range. Conversely, inner sandy areas and the 5 km buffer zones of the oasis, which reached up to 50 °C, were classified as extreme dangerous. Various reclassification methods were tested, and Natural Breaks produced values that closely matched these observations. Intermediate values were compared to the real cases and found suitable.

The safety levels for NDVI were determined based on field observation. NDVI values up to 0.1 were indicative of nearly plantless areas in the buffer zone and inner sandy regions, while values between 0.1 and 0.3 indicated the presence of sparse vegetation, such as a few trees, shrubs, and grasses (Table 4). The safe NDVI areas were found to correspond with the safe areas for LST, soil brightness, and NDWI (Figure 4e). Intermediate NDVI safety levels were observed to be variable and subject to change over time.

NDMI values are widely acknowledged as a key indicator for drought detection (Gu et al., 2008; Assal et al., 2016), with notable regional variations. It should be noted that not all NDMI values were present in the oasis. Consequently, the safety levels for this factor were selected on a conditional basis and compared with NDVI, LST, and other factors. The Natural break reclassification method was employed, with adjustments based on filed observations. Values between 0.13 and 0.27 were indicative of areas of intensive agriculture, and were thus considered safe. NDMI values with –0.2 to 0.007 idexes indicated sparse vegetation, and dry conditions or weak vegetation.

NDMI values between 0.05 and 0.09 are indicative of inner sandy areas with minimal vegetation and unused agricultural fields with a sparse vegetative cover (Figure 4f).

The AMGWT proved to be a significant contributor to mitigation of the adverse effects of the drought. The AMGWT was employed extensively during the drought years 2000, 2001, 2008, and 2016 to support local harvest. Furthermore, it facilitated the formation of lakes, wetlands, and natural vegetation cover. The establishment of safety levels for this factor was informed by traditional and practical knowledge (Figure 4g). A depth of up to 1.5 meters was deemed safe from drought, but posed challenges due to high salinity for agricultural, construction and road purposes (Matchanov, 2021). AMGWT was subject to a number of influencing factors, including proximity to the Tuyamuyun water reservoir, the Amudarya River, density of main canals, and local agricultural practices. By way of illustration, the depth ranged from 0.87 to 1.5 metres in Khorezm and from 3.5 to 5 metres in the vicinity of the Aral Sea. The Tuyamuyin reservoir, constructed at an elevation of 130 meters above the sea level, provided irrigation water for the oasis. The AMGWT, exhibited a decline with increasing distance from the elevation in question, a phenomenon that can be attributed to anthropogenic influences. This resulted in a negative correlation between DEM and AMGWT, as deeper water tables were formed even below sea level. Furthermore, the AMGWT was manually lowered around cities like Urgench and Khiva for structural protection. The safety level for DEM was set using equal intervals (Figure 4h). The Ustyurt hills, Sulton Uvays eroded mountains, and some other hills were identified as safe areas from drought but did not significantly affect the overall results due to their buffer zone location.

A variety of statistical methodologies exist for the purpose of weight assessment. In this study, weights were assigned based on field observations, comparative judgment, and expert evaluations. A multitude of weight value combinations were tested, with adjustments continuing until the pixel values aligned with field observation data. The control points consisted of three groups of land areas. The first group included agricultural fields that consistently received irrigation water without experiencing shortages in any given year. These points were initially identified through a farmer questionnaire on irrigation water availability. Subsequent field observations, particularly during drought years, were conducted to verify the data. Once all first-group control fields were classified within the safe zone, the final weight value combinations were determined.

The second group consists of agricultural fields where irrigation water is available until June in any given year. After this month, irrigation water becomes unavailable, and farmers resort to using groundwater to protect the crops. However, once groundwater is depleted, the fields are left fallow during the summer. More than 90% of the high-risk areas fall into this group.

The third group consists of desert transition and desert areas, which include the most hazardous and extremely dangerous regions. Medium and high-risk areas appeared in an irregular spatial pattern and became evident once the conditions for the previous three groups were met. Based on expert evaluations, the following weight values

Table 4. Safety levels for NDVI

Safety levels	NDVI	Description	Grades
Safe	0.7–1	Dens and high trees, gardens, shrubs, dens and irrigated agri-fields, lakes, wetlands, and their surroundings with natural reeds	5
Dangerous	0.5–0.7	Mid-dense and high trees, gardens, dense shrubs and grasses, agricultural fields	4
Mid-dangerous	0.3–0.5	Rare and high trees, shrubs and grasses, agricultural fields	3
High-dangerous	0.1–0.3	Very rare trees, shrubs and grasses	2
Extreme-dangerous	–0.062–0.1	Almost plantless areas	1

were assigned: Distance from the river 0.2, canal density 0.18, soil brightness 0.15, LST 0.13, annual groundwater table 0.11, NDVI 0.09, NDMI 0.08, and DEM 0.06. These weights were calculated using the weighted overlay equation (Rahman et al., 2014).

$$R_{eq} = \sum_{i=1}^{n} w_i \times x_i,$$

where R_{eq} – drought condition, w_i – weight factor of $_i$, and x_i –criterion score of factor $_i$, and $_n$ is the total number of factors. The final result was the drought safety levels assessment map created and it was given Figure 5.

3.3. Discussions

The safe areas on the left banks of the Amudarya, protected from drought risk, covered 3746 km^2 and mainly found in the Khorezm 2352.59 km^2 (Table 5). This was due to anthropogenic factors. Farmers applied greater quantities of irrigation water, and the soil fertility and quality scores were higher in this region. This pattern persisted even during the drought years of 2000 and 2001. The safe areas within 10 km of the river showed a continuous distribution and extended around the main canals, with only a small area present in the Karakalpakstan part of the oasis.

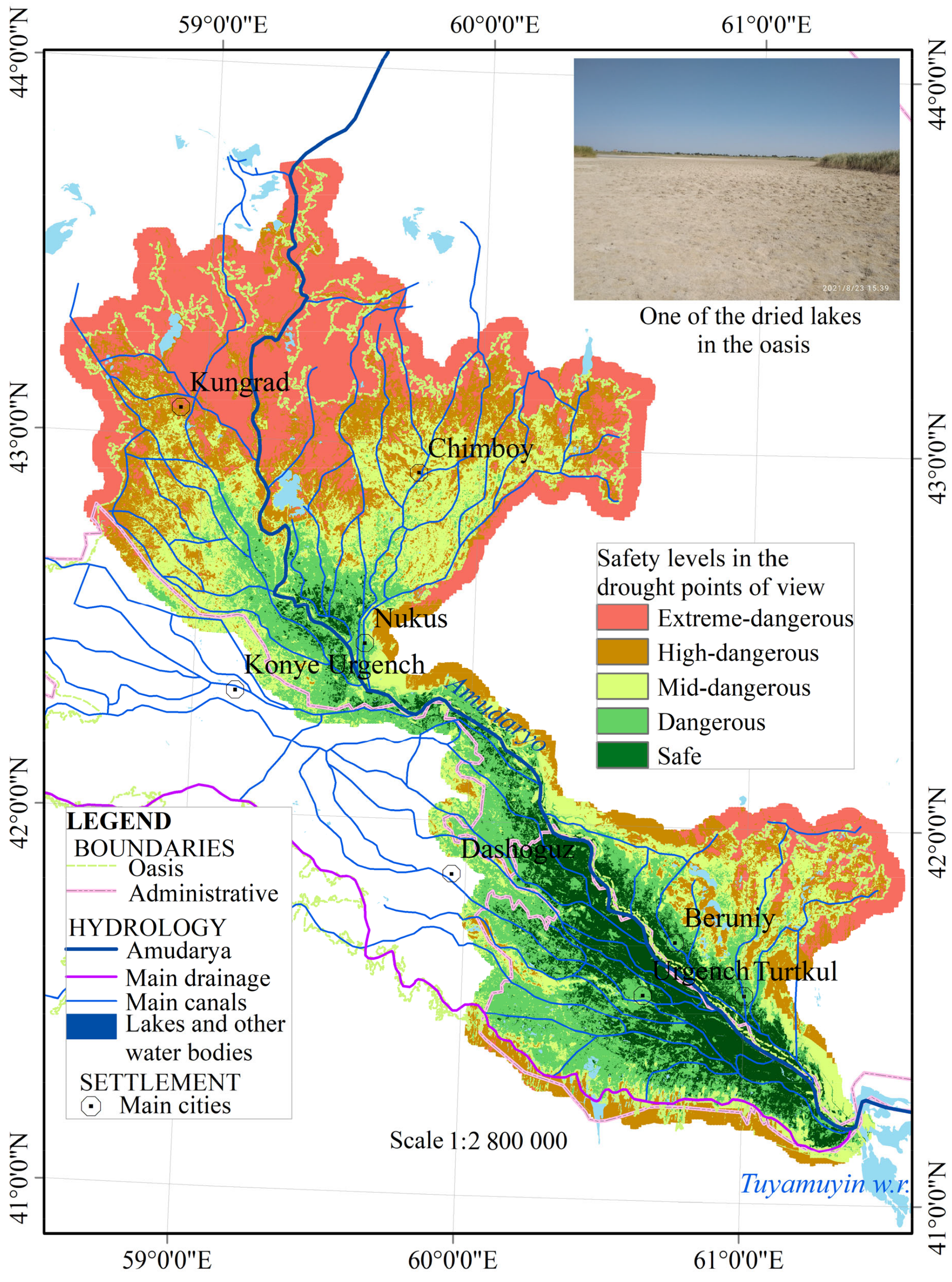

Figure 5. The drought safety levels assessment map of the Khorezm oasis

Table 5. The safety levels in the drought point of view in the oasis administrative parts

Safety levels	Total	Karakalpakstan	Khorezm	Buffer area
Safe	3746.0	1139.15	2352.59	254.26
Dangerous	4644.32	2484.61	1426.19	333.52
Mid-dangerous	5563.77	3974.16	328.59	1261.02
High-dangerous	5486.17	3682.5	62.18	1741.4
Extreme-dangerous	7832.64	2894.51	0	4938.13

Policy and practice implications of the results: The government exercises control over the designated safe area, utilising it in a strategic manner for wheat production. The implementation of crop rotation with vegetables could prove advantageous. It would be prudent to restrict the use of land for residential, commercial, and other purposes, in order to safeguard agricultural lands. This area is sufficiently expansive to produce the annual wheat harvest required by the oasis population.

The total dangerous area was 4644.32 km^2, with 2484.61 km^2 situated within the Karakalpakstan portion of the oasis. This region formed in the southern areas of the Khorezm region (1426.19 km^2). The dangerous region is prone to drought and is characterised by inconsistent irrigation water supply, which has resulted in instability. The lack of an early warning system meant that the region faced a significant risk of severe drought impacts. Farmers and dehkans used their lands for agricultural purposes, but drought typically began after mid-May due to a range of analysed factors. For instance, in wheat cultivation, mid-May coincided with winter wheat flowering and a reduction in river water supply. Water needs were met using drainage, lakes, and underground sources, which led to costly harvesting efforts and soil degradation from saline water. Due to necessity, people accepted these risks.

The implementation of drip irrigation, a common practice in regions such as Andalusia in Spain is recommended for the cultivation of apricots, apples, and Elaeagnus L. in the oasis. While residential, commercial, and other land use should be permitted, they must adhere to established restrictions.

A region of Mid-dangerous, spanning 5563.77 km^2, was identified, with a significant portion situated within the Karakalpakstan portion of the oasis. This region was characterised by sparse vegetation and land utilised for non-permanent agricultural activities. Only the southern regions of the Khorezm area exhibited mid-dangerous encompassing 328.59 km^2. These regions were recommended for utilisation in animal husbandry, with regular scientific monitoring.

High and extremely high dangerous areas were identified in the buffer zone, the inner sandy regions, and predominantly in the northern parts of Karakalpakstan. The areas designated as extreme-high dangerous areas were situated entirely within the Karakalpakstan region of the oasis, encompassing a total area of 2894.51 km^2. The total high-dangerous area was 5486.17 km^2, and 3682.5 km^2 located in the Karakalpakstan region (Table 5). This increase in dangerous level was linked to the decreasing Amudarya water levels over the years, which heightened the risk of drought, as confirmed by previous research (Matchanov et al., 2016). These areas required ecological protection and no land-use activities were recommended. The region was highly vulnerable to desertification, and it was suggested that the population be gradually relocated to more ecologically stable areas of the country.

4. Conclusions

The oasis has been experiencing drought issues since the 1960s, yet no scientific-based strategies have been developed by the government to address the negative impacts of this phenomenon. Furthermore, recent shifts in the geopolitical landscape of Central Asian have prompted alterations in the governance of transboundary river water resources, with the Kushtepa canal in Afghanistan serving as a case in point. The methodology proposed in this study for assessing the safety of oases in the event of drought can be employed to develop more effective plans for their preparation for such an eventuality.

The indicators examined in this study, along with their proposed weights were analysed in a variety of combinations. These factors exert a direct influence on one another in different parts of the oasis at varying levels. However, the distance from the river and the density of the main canals were identified as the primary factors influencing the drought safety levels in the region.

To mitigate the negative impacts of drought, it is imperative that early warning systems are developed. This would assist in optimising the use of agricultural land in the dangerous areas of the oasis. It is incumbent upon the government to take immediate action to gradually relocate populations from high-dangerous areas and to implement more effective management of agricultural activities in safer zones, with the aim of ensuring food security.

Acknowledgements

The corresponding author thanks for all the workers of hydrogeological stations in Khorezm, Uzbekistan and Karakalpakstan republics who assisted with underground water data collection.

Funding

This research received no external funding.

Author contributions

Professor Matías Mudarra and Professor Askar Nigmatov were the main experts and advisors. Conceptualization, supervision, methodology, software, validation, formal analysis, investigation, and writing the original and draft preparation done by Dr. Muzaffar Matchanov. Rifat Boymurodov, Ruslan Jumabayev, and Otabek Matchanov were responsible for data collection, the field data truth and analysis. Ali Hakimi was responsible for English editing, revisions and data interpretation.

Disclosure statement

All the authors declare they do not have any competing financial, professional, or personal interests from other parties.

References

Assal, T. J., Anderson, P. J., & Sibold, J. (2016). Spatial and temporal trends of drought effects in a heterogeneous semi-arid forest ecosystem. *Forest Ecology and Management*, *365*, 137–151. https://doi.org/10.1016/j.foreco.2016.01.017

Baniya, B., Tang, Q., Xu, X., Haile, G. G., & Chhipi-Shrestha, G. (2019). Spatial and temporal variation of drought based on satellite-derived Vegetation Condition Index in Nepal from 1982–2015. *Sensors*, *19*(2), Article 430. https://doi.org/10.3390/s19020430

Boymurodov, R., Matchanov, M., Tajiyev, Q., Amandurdiyev, D., Mansourian, A., & Ashurov, A. (2024). Monitoring land use and land cover (LULC) in the Khorezm Oasis using the ESRI Sentinel-2 Land Cover Explorer database. *E3S Web of Conferences*, *590*, Article 04001. https://doi.org/10.1051/e3sconf/202459004001

Brown, J. F., Wardlow, B. D., Tadesse, T., Hayes, M. J., & Reed, B. C. (2008). The Vegetation Drought Response Index (VegDRI): A new integrated approach for monitoring drought stress in vegetation. *GIScience & Remote Sensing*, *45*(1), 16–46. https://doi.org/10.2747/1548-1603.45.1.16

Chen, X., Tian, F., & Su, Y. (2022). How did the late 1920s drought affect northern Chinese society? *Weather and Climate Extremes*, *36*, Article 100451. https://doi.org/10.1016/j.wace.2022.100451

Climate Engine. (2023). *Desert Research Institute and University of California, Merced*. http://climateengine.org

Crippen, R. E. (1990). Calculating the vegetation index faster. *Remote Sensing of Environment*, *34*(1), 71–73. https://doi.org/10.1016/0034-4257(90)90085-Z

Das, A., Shahriar, S. A., Chowdhury, M. A., Hossain, M., Mahmud, S., Tusar, M. K., Ahmed, R., & Salam, M. (2023). Assessment of remote sensing-based indices for drought monitoring in the north-western region of Bangladesh. *Heliyon*, *9*(6), Article e13016. https://doi.org/10.1016/j.heliyon.2023.e13016

Dubey, A., Swami, D., Gupta, V., & Joshi, N. (2023). From the peaks to the plains: Investigating the role of elevation in governing drought dynamics over the Indus River Basin. *Atmospheric Research*, *291*, Article 106824. https://doi.org/10.1016/j.atmosres.2023.106824

Gao, B.-C. (1996). NDWI–A normalized difference water index for remote sensing of vegetation liquid water from space. *Remote Sensing of Environment*, *58*(3), 257–266. https://doi.org/10.1016/S0034-4257(96)00067-3

Getis, A., & Ord, J. K. (1992). The analysis of spatial association by use of distance statistics. *Geographical Analysis*, *24*(3), 189–206. https://doi.org/10.1111/j.1538-4632.1992.tb00261.x

Gonçalves, S., Vasconcelos, F. C., Jr., Silveira, C. S., Cid, D. A., Martins, E. S. P. R., & Costa, J. E. (2023). Comparative analysis of drought indices in hydrological monitoring in Ceará's semi-arid basins, Brazil. *Water*, *15*(7), Article 1259. https://doi.org/10.3390/w15071259

Gorelick, N., Hancher, M., Dixon, M., Ilyushchenko, S., Thau, D., & Moore, R. (2017). Google Earth Engine: Planetary-scale geospatial analysis for everyone. *Remote Sensing of Environment*, *202*, 18–27. https://doi.org/10.1016/j.rse.2017.06.031

Gu, Y., Hunt, E., Wardlow, B., Basara, J. B., Brown, J. F., & Verdin, J. P. (2008). Evaluation of MODIS NDVI and NDWI for vegetation drought monitoring using Oklahoma Mesonet soil moisture data. *Geophysical Research Letters*, *35*(22), Article L22401. https://doi.org/10.1029/2008GL035772

Hao, Z., Yuan, X., Xia, Y., Hao, F., & Singh, V. P. (2017). An overview of drought monitoring and prediction systems at regional and global scales. *Bulletin of the American Meteorological Society*, *98*(9), 1879–1896. https://doi.org/10.1175/BAMS-D-15-00149.1

Hosseinzadehtalaei, P., Van Schaeybroeck, B., Termonia, P., & Tabari, H. (2023). Identical hierarchy of physical drought types for climate change signals and uncertainty. *Weather and Climate Extremes*, *41*, Article 100573. https://doi.org/10.1016/j.wace.2023.100573

Jang, D. (2018). Assessment of meteorological drought indices in Korea using RCP 8.5 scenario. *Water*, *10*(3), Article 283. https://doi.org/10.3390/w10030283

Li, F., Jackson, T. J., Kustas, W. P., Schmugge, T. J., French, A. N., Cosh, M. H., & Bindlish, R. (2004). Deriving land surface temperature from Landsat 5 and 7 during SMEX02/SMACEX. *Remote Sensing of Environment, 92*(4), 521–534. https://doi.org/10.1016/j.rse.2004.02.018

Lloyd-Hughes, B. (2014). The impracticality of a universal drought definition. *Theoretical and Applied Climatology*, *117*(3–4), 607–611. https://doi.org/10.1007/s00704-013-1025-7

Mansourian, A., Matchanov, M., Farnaghi, M., & Pilesjö, P. (2023). Chapter 12 – iMSEP: A GIT-based digital solution for disaster management. In J. F. Shroder, P. Paron, & G. Di Baldassarre (Eds.), *Hydro-meteorological hazards, risks, and disasters* (2nd ed., Vol. 5, pp. 323–334). Elsevier. https://doi.org/10.1016/B978-0-12-819101-9.00012-1

Matchanov, M. (2020). Comparison ASTER, SRTM and GOOGLE DEM with ground data in a small-scale agricultural land. *Journal of Agricultural Science*, *10*(5), 288–395.

Matchanov, M. (2021). *Ecological safety and its physical geographical aspects (in the case of Khorezm region)*. Quvonchbek-Mashhura.

Matchanov, M., Teodoro, A., & Schröder, C. (2016). Criterion definition for the identification of physical-geographical boundaries of Khorezm Oasis through remotely sensed data. *Environmental Monitoring and Assessment*, *188*(1), Article 35. https://doi.org/10.1007/s10661-015-5035-z

McKee, T. B., Doesken, N. J., & Kleist, J. R. (1993). *The relationship of drought frequency and duration to time scales*. 8th Conference on Applied Climatology, Anaheim, California.

Mirmohammad Hosseini, T., Hosseini, S. A., Ghermezcheshmeh, B., & Sharafati, A. (2020). Drought hazard depending on elevation and precipitation in Lorestan, Iran. *Theoretical and Applied Climatology*, *142*(3–4), 1369–1377. https://doi.org/10.1007/s00704-020-03386-y

NASA JPL. (2020). *NASA Shuttle Radar Topography Mission Global 1 arc second* [Data set]. NASA EOSDIS Land Processes DAAC. https://doi.org/10.5067/MEaSUREs/SRTM/SRTMGL1.003

Patil, A., Patil, A., Somnath, P., Sushant, S., Shital, K., & Panhalkar, S. (2021). Analysis of the agriculture drought severity and spatial extent using Vegetation Health Index (VHI) in Manganga watershed of Maharashtra, India. *Disaster Advances*, *14*(5), 36–47.

Raczynski, K., & Dyer, J. (2022). Variability of annual and monthly streamflow droughts over the southeastern United States. *Water*, *14*(23), Article 3848. https://doi.org/10.3390/w14233848

Rahman, M. M., Shi, Z.-H., & Chongfa, C. (2014). Assessing regional environmental quality by integrated use of remote sensing, GIS, and spatial multi-criteria evaluation for prioritization of environmental restoration. *Environmental Monitoring and Assessment*, *186*(10), 6993–7009. https://doi.org/10.1007/s10661-014-3905-4

Salleh, S. A., Latif, Z. A., Pradhan, B., Wan Mohd, W. M. N., & Chan, A. (2014). Functional relation of land surface albedo with climatological variables: A review on remote sensing techniques and recent research developments. *Geocarto International*, *29*(2), 147–163. https://doi.org/10.1080/10106049.2012.748831

Schneider, K., & Mauser, W. (1996). Processing and accuracy of Landsat Thematic Mapper data for lake surface temperature measurement. *International Journal of Remote Sensing*, *17*(11), 2027–2041. https://doi.org/10.1080/01431169608948757

Shah, D., & Mishra, V. (2020). Integrated Drought Index (IDI) for drought monitoring and assessment in India. *Water Resources Research*, *56*(6), Article e2019WR026284. https://doi.org/10.1029/2019WR026284

Tajudin, N., Ya'acob, N., Mohd Ali, D., & Adnan, N. (2021). Soil moisture index estimation from Landsat 8 images for prediction and monitoring landslide occurrences in Ulu Kelang, Selangor, Malaysia. *International Journal of Electrical and Computer Engineering*, *11*(3), 2101–2108. https://doi.org/10.11591/ijece.v11i3.pp2101-2108

Van Loon, A. F., Rangecroft, S., Coxon, G., Werner, M., Wanders, N., Di Baldassarre, G., Tijdeman, E., Bosman, M., Gleeson, T., Nauditt, A., Aghakouchak, A., Breña-Naranjo, J. A., Cenobio-Cruz, O., Costa, A. C., Fendekova, M., Jewitt, G., Kingston, D. G., Loft, J., Mager, S. M., & Van Lanen, H. A. J. (2022). Streamflow droughts aggravated by human activities despite management. *Environmental Research Letters*, *17*(4), Article 044059. https://doi.org/10.1088/1748-9326/ac5def

Wang, S., Davidson, A., & Latifovic, R. (2004). Impact of drought on land surface albedo. *AGU Spring Meeting Abstracts*, *2004*, H31C-03.

Wilhite, D. A., & Glantz, M. H. (1985). Understanding the drought phenomenon: The role of definitions. *Water International*, *10*(3), 111–120. https://doi.org/10.1080/02508068508686328

Wu, J., Zhou, L., Liu, M., Zhang, J., Leng, S., & Diao, C. (2013). Establishing and assessing the Integrated Surface Drought Index (ISDI) for agricultural drought monitoring in mid-eastern China. *International Journal of Applied Earth Observation and Geoinformation*, *23*, 397–410. https://doi.org/10.1016/j.jag.2012.11.003

Yao, Y., Qin, Q., Zhu, L., & Yang, N. (2008). Relationship between surface albedo, vegetation index, and surface dryness using Landsat ETM+ imagery. *IGARSS 2008 – 2008 IEEE International Geoscience and Remote Sensing Symposium*, *1*, 315–318. https://doi.org/10.1109/IGARSS.2008.4778856

Zarei, A. R. (2018). Evaluation of drought condition in arid and semi-arid regions, using RDI index. *Water Resources Management*, *32*(5), 1689–1711. https://doi.org/10.1007/s11269-017-1898-9